CHEMICAL ENGINEERING TRANSACTIONS
VOL. 117, 2025
A publication of AIDIC
The Italian Association of Chemical Engineering
Online at www.cetjournal.it
Guest Editors: Fabrizio Bezzo, Flavio Manenti, Gabriele Pannocchia, Almerinda di Benedetto
Copyright © 2025, AIDIC Servizi S.r.l.
ISBN 979-12-81206-17-5; **ISSN** 2283-9216
DOI: 10.3303/CET25117090

Bio-Polyurethane based Nanocomposites Membranes: Synthesis and Characterization

Elda X. S. Silveira*, Maria Ingrid R. B. Schiavon, Bruno A. B. Francisco, Gustavo Doubek, Rubens Maciel Filho

University of Campinas, School of Chemical Engineering, Av. Albert Einstein, 500. Campinas, SP, Brazil, 13083-852
elda.silveira1@gmail.com

Biopolymer-based nanocomposites are an alternative to replace petroleum-based polymers due to their user-friendliness, biodegradability, abundance, and non-toxicity. Additionally, polymers derived from natural resources have the potential to align with the principles of a circular economy. Castor oil, a natural, non-toxic, and inedible compound, offers numerous advantages, including low cost, abundant availability, and non-competition with food production. In this study, bio-polyurethane (BPU) nanocomposite membranes were synthesized via in situ polymerization using castor oil, 4,4-diphenylmethane diisocyanate (MDI), 1,4-butanediol (BD), glycerine (Gly), and fumed silica (SiO_2) nanoparticles, with varying silica concentrations (0%, 0.5%, and 1%). The membranes were characterized in terms of surface morphology, cross-sectional structure, pore size distribution, surface area, water contact angle, and were compared with commercial polypropylene (PP) membranes. The results showed that while PP membranes exhibited a normal distribution of micropores, mesopores, and macropores, the BPU nanocomposite membranes only contained mesopores. Furthermore, the maximum pore size of the BPU nanocomposite membrane containing 1.0% SiO_2 was reduced by more than 80% compared to the membrane containing 0.5% nanoparticles. This work characterizes the structure of a new membrane synthesized from a renewable resource and assesses the effect of silica addition in the characteristics of the membrane as potential substitutes for fossil-derived membranes.

1. Introduction

Polymer nanocomposites demonstrate a broad spectrum of applications, including pharmaceuticals, agriculture, sports, and electronics. The incorporation of nanoparticles into polymer matrices not only improves key properties of pure polymers, such as elasticity, durability, barrier performance, solvent and thermal resistance, and flame retardancy, but also imparts novel functionalities depending on the specific nanomaterials employed (Khan et al., 2022). This approach addresses the inherent limitations of pure polymers, as nanostructures alter surface properties and fine-tune the physicochemical characteristics of the matrix, directly influencing the performance of the resulting composites (Assad et al., 2023).

Silica nanoparticles have attracted significant attention due to their ease of production and diverse industrial applications. Their size and distribution greatly influence product performance, and studies show that incorporating small amounts of nanoparticles into polymers enhances mechanical, thermal, electrical, photonic, and gas barrier properties (Bakhtiar et al., 2022).

Bio-based polymers are biodegradable materials derived from renewable biomass sources (Kumar et al., 2023) and offer ecological advantages, including reduced carbon footprint, waste management, and high recycling potential, playing a crucial role in the bioeconomy. These polymers are utilized in the development of biofilms, fibers, membranes, blends, composites, and nanocarriers (Zia et al., 2021). Among renewable resources, vegetable oils are highly promising, capable of direct chemical modification and functionalization. They consist of triglycerides, molecules with a triester of fatty acids (Rajput et al., 2023).

Due to its simple structure, widespread availability, abundant active sites, low toxicity, cost-effectiveness, and industry suitability, castor oil has emerged as one of the rapidly growing commercial vegetable oils with several studies identifying castor oil as a potential polyol source to substitute petroleum-derived products (Ma et al.,

Paper Received: 1 January 2025; Revised: 2 March 2025; Accepted: 6 May 2025
Please cite this article as: Silveira E.X., Schiavon M.I.R.B., Francisco B.A., Doubek G., Maciel Filho R., 2025, Bio-polyurethane Based Nanocomposites Membranes: Synthesis and Characterization, Chemical Engineering Transactions, 117, 535-540 DOI:10.3303/CET25117090

2024). Castor oil distinguishes itself from other vegetable oils by being non-edible, non-competition with food and, as a natural polyol, is utilized in polyurethane synthesis (Nekhavhambe et al., 2019). Polyurethanes (PUs) can be synthesized through a polyaddition reaction between the hydroxyl groups (–OH) of polyols and the isocyanate functional groups (–N=C=O). By varying the types and amounts of polyol and isocyanate, polyurethanes with diverse properties can be obtained (Asare et al., 2022).
In this context, bio-polyurethane (BPU) nanocomposite membranes with different concentrations of SiO_2 nanoparticles were developed. These membranes were characterized in terms of surface morphology, cross-sectional structure, pore size distribution, surface area, and water contact angle. Comparative analyses were performed against commercial polypropylene (PP) membranes to assess their potential as substitutes for fossil-derived membranes.

2. Method

2.1 Synthesis of BPU nanocomposite membranes

BPU nanocomposites were synthesized by in situ polymerization under an inert nitrogen atmosphere, using castor oil as the bio-polyol, 4,4'-diphenylmethane diisocyanate (MDI) as the isocyanate, and a chain extender blend consisting of 60:40 1,4-butanediol (BD) and glycerine (Gly) in a molar ratio of 2:1:1. Silica nanoparticles were incorporated at concentrations of 0.0%, 0.5%, and 1.0% by weight. Initially, castor oil, with a molecular mass of 933.4 g/mol, was dried at 70 °C under vacuum conditions. Subsequently, MDI was incorporated into the dried castor oil and stirred at 80 °C for 1 hour to facilitate the formation of a prepolymer. Afterward, silica nanoparticles were introduced into the prepolymer mixture, followed by the addition of 1,4-butanediol and glycerine. The resulting bio-polyurethane, synthesized in the presence of silica nanoparticles, was then applied onto a cellulose substrate (70 mm diameter, 80 g) using a Spin Coater (Chemat Technology, KW-4A, Northridge, USA) at a rotational speed of 5000 rpm to form the BPU nanocomposite membranes.

2.2 Characterization of BPU nanocomposite membranes

The morphology and thickness of the membranes were analyzed using scanning electron microscopy (SEM) (Quattro S, Thermo Fisher Scientific, Brno, Czech Republic). To enhance the image resolution, gold (Au) particles were sputtered onto the membrane surface using a sputter coater (Emitech K450, Kent, UK). The SEM equipment is coupled with a Leo 440i detector for energy-dispersive X-ray spectroscopy (EDS) (ANAX-60P-B, Thermo Scientific UltraDry, Brno, Czech Republic), which was employed to map the distribution of silica nanoparticles within the membranes. Nitrogen adsorption and desorption isotherms, surface area, and pore size distribution were determined using an Accelerated Surface Area and Porosimetry System (ASAP 2020 Plus, Micromeritics, Norcross, USA). The hydrophobic/hydrophilic properties of the membranes were evaluated using a Drop Shape Analyzer (DSA100, Krüss, Hamburg, German), with the contact angle measured at the moment the water droplet was first applied.

3. Results and Discussion

Figure 1 depicts the surface morphology (at different magnifications) and thickness of BPU nanocomposite membranes with different silica concentrations (0%, 0.5%, and 1%), compared to a commercial polypropylene (PP) membrane. The morphology of the BPU membrane without silica (Figure 1a, e) appears relatively smooth, indicating a homogeneous polymer matrix. The membranes containing 0.5% silica (Figure 1b, f) and 1.0% silica (Figure 1c, g) exhibited surface morphologies similar to that of the membrane without silica. The surface of the PP membrane (Figure 1d, h) shows a distinct fibrous, web-like structure, indicating a more porous or fiber-oriented organization. The cross-sectional images (Figure 1i to l) reveal both membrane thickness and internal structure. The BPU membranes (Figure 1i, j, k) have a similar thickness of approximately 120 µm, but their internal microstructure appears more complex, with distinct layers and interfaces and the fibers appear to be more porous with the increase of silica content. In contrast, the PP membrane is significantly thinner (around 23 µm) and presents a different internal structure, likely due to its fibrous, more oriented morphology (DeMeuse, 2021) compared to the BPU membranes.
The distribution of silica in the membranes (indicated by the green coloration in the images) is shown in Figure 2. The BPU nanocomposite with 0.5% silica (Figure 2a) exhibited a uniform silica dispersion within the polymer matrix. In contrast, a denser silica distribution was observed in the BPU nanocomposite with 1.0% silica (Figure 2b), suggesting that the higher silica concentration leads to the formation of larger silica agglomerates.
Figure 3 illustrates the nitrogen adsorption-desorption isotherms and the surface areas calculated using the BET (Brunauer-Emmett-Teller) method for the membranes. The BPU nanocomposite with 0.0% silica isotherm (Figure 3a) exhibited behavior typical of mesoporous materials, with a gradual increase in the adsorbed quantity at intermediate relative pressures, followed by a sharp increase at high relative pressures ($P/P_0 \approx 1$) (Nishi &

Inagaki, 2016). The presence of hysteresis between the adsorption and desorption curves suggests the existence of pores that are not fully accessible, characteristic of cylindrical or bottle-neck-shaped pores (Kyzas & Mitropoulos, 2018). The behavior of the membrane with 0.5% silica (Figure 3b) is similar to the membrane without silica, including the adsorbed volume (<0.5 cm^3/g) and the BET surface area (~0.6 m^2/g). The hysteresis loop persists, indicating that the porous morphology remains relatively unchanged. For the membrane with 1.0% silica (Figure 3c), the adsorbed quantity is noticeably lower (<0.2 cm^3/g), suggesting that the higher concentration of silica may have led to partial pore blockage or the formation of silica aggregates (as noted in Figure 2b), reducing the accessible surface area (BET surface area with 1.0% silica = 0.3052 m^2/g). The hysteresis loop appears slightly different when compared to the other membranes, which may indicate a change in pore structure, possibly with fewer mesopores or a different pore shape. The polypropylene isotherm (Figure 3d) shows a distinct shape, with higher adsorption at high relative pressures, typical of macroporous materials (Anovitz & Cole, 2015). The almost vertical isotherm at maximum relative pressure ($P/P_0 \approx 1$) indicates limited adsorption at lower relative pressures and rapid capillary condensation in macropores at high pressures (Zhang et al., 2016). Furthermore, the BET surface area is higher than that of the BPU nanocomposites (27.6170 m^2/g), which can be attributed to its more porous structure (as noted in Figure 1h).

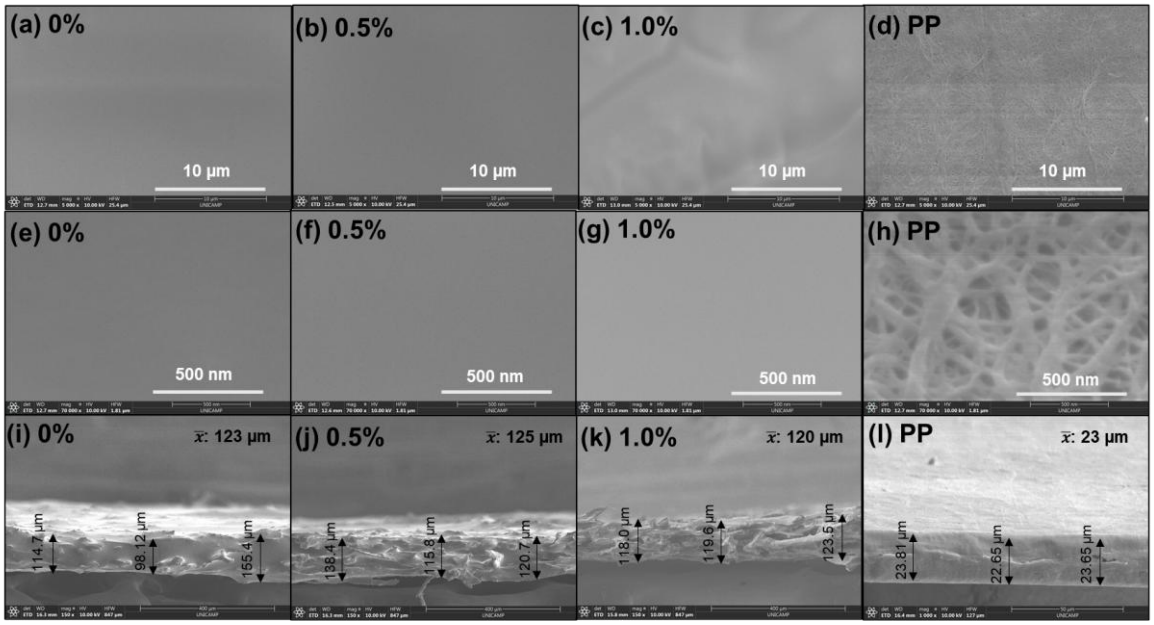

Figure 1: Images at low and high magnifications (x5 k and x70 k) and thickness of the membranes: (a, e, i) BPU nanocomposite with 0.0% silica; (b, f, j) BPU nanocomposite with 0.5% silica; (c, g, k) BPU nanocomposite with 1.0% silica; and (d, h, l) polypropylene (PP), respectively.

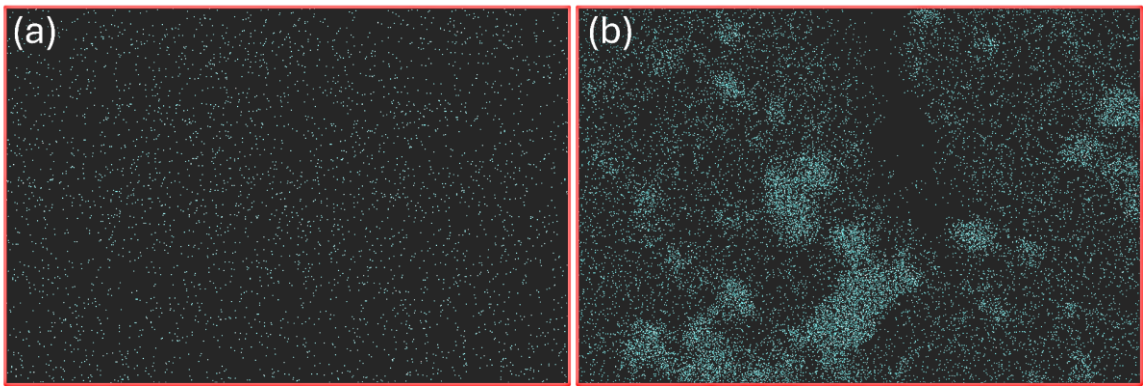

Figure 2: Map of silica distribution in the membranes. (a) BPU nanocomposite with 0.5% nanosilica and (b) BPU nanocomposite with 1.0% silica.

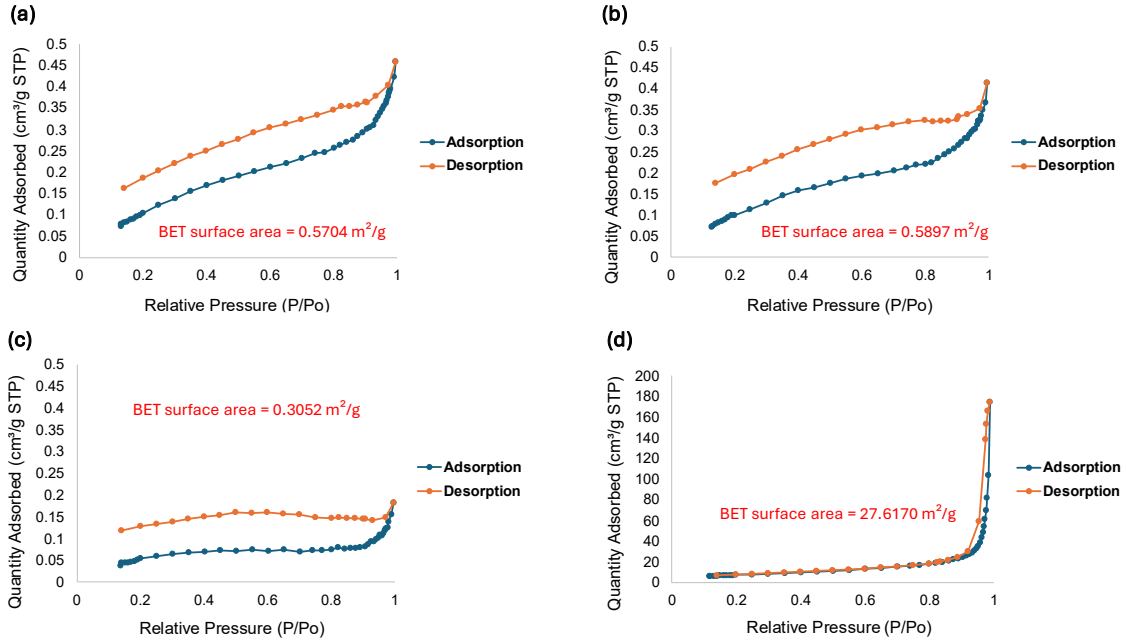

Figure 3: Nitrogen adsorption-desorption isotherms at 77 K and the BET surface area. (a) BPU nanocomposite with 0.0% silica. (b) BPU nanocomposite with 0.5% silica. (c) BPU nanocomposite with 1.0% silica. (d) polypropylene (PP).

The BJH (Barrett-Joyner-Halenda) method was applied to determine the pore size distribution of the membranes (Figure 4). Data were obtained from the BJH Desorption Pore Distribution Report generated by the ASAP 2020 Plus system. The pores of the BPU nanocomposite membranes (Figures 4a to 4c) fall within the mesoporous range. However, the BPU nanocomposite without silica (Figure 4a) and the composite with 0.5% silica (Figure 4b) exhibit a maximum pore diameter of approximately 36 nm, with a gradual decrease in pore volume as the diameter reduces to around 15 nm. This suggests that low silica content induces minimal changes in the overall porosity distribution. In contrast, the BPU nanocomposite with 1.0% silica (Figure 4c) shows pores concentrated between 2 to 4 nm, with a reduced pore volume. This indicates that higher silica concentrations either fill or disrupt pore formation, leading to a denser matrix with fewer accessible pores, potentially decreasing the porosity of the membrane (Alothman, 2012). The polypropylene membrane (Figure 4d) presents a distinct structure, with a broad pore size distribution spanning micro, meso, and macropores, and a significantly higher pore volume, particularly in the meso and macropore regions. This suggests that polypropylene exhibits a predominantly macroporous structure, contrasting with the denser matrix of the BPU nanocomposites.

Figure 5 shows the water contact angle measurements for the membranes. The incorporation of 0.5% silica into the polyurethane matrix increased the hydrophobicity of the composite material (Figure 5b) compared to the BPU nanocomposite without silica (Figure 5a). This enhancement in hydrophobicity is attributed to the silica nanoparticles reducing the surface energy of the polymer matrix, thereby decreasing its affinity for water (Singh & Singh, 2022). The improved hydrophobicity properties arise from the surface characteristics of the silica nanoparticles and their interaction with the polymer matrix, resulting in changes in surface roughness and increased water repellency (Tripathi et al., 2024). However, the hydrophobicity of the BPU nanocomposite with 1.0% silica (Figure 5c) decreased. This observation suggests that the dispersion of silica within the polymer matrix significantly affects this property. As highlighted in Figure 2, higher silica concentrations in the polyurethane matrix result in particle agglomeration, which may reduce the effective interaction between silica and the polymer matrix, thereby diminishing the hydrophobic effect. The polypropylene membrane (Figure 5d) exhibited higher hydrophobicity compared to the other membranes, attributed to its chemical and physical properties, including non-polar hydrocarbon chains with strong C-H and C-C bonds (Gilbert, 2017).

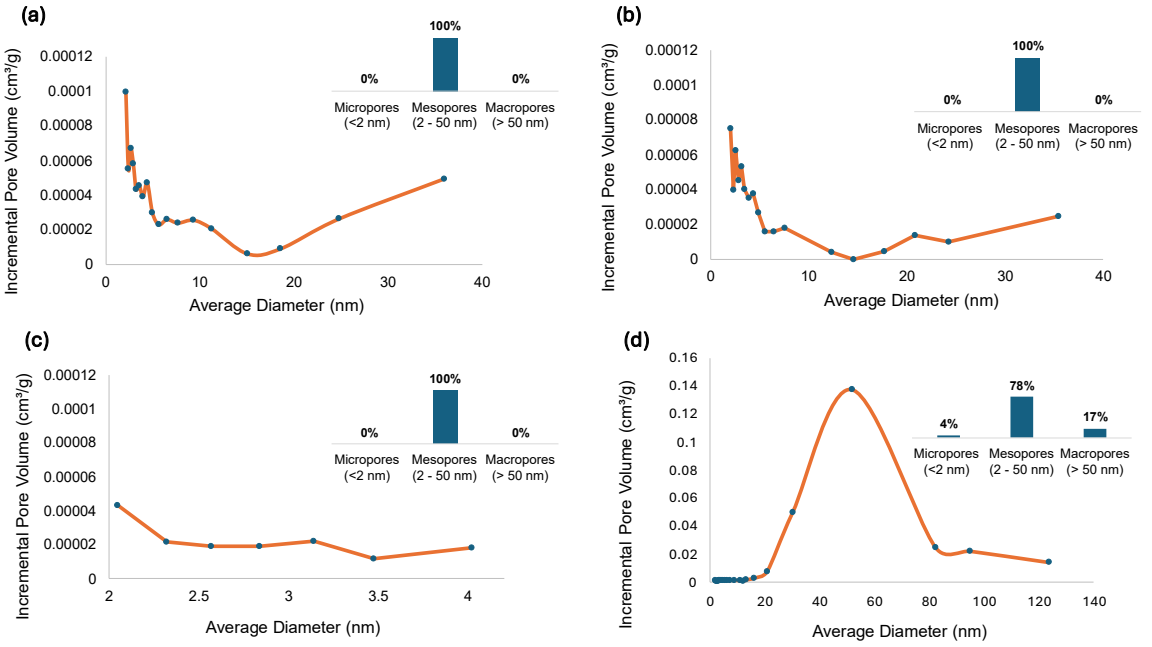

Figure 4: Pore size distribution at BJH desorption. (a) BPU nanocomposite with 0.0% silica; (b) BPU nanocomposite with 0.5% silica; (c) BPU nanocomposite with 1.0% silica; and (d) polypropylene (PP).

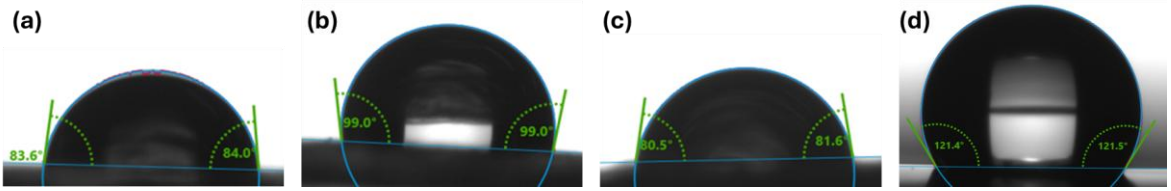

Figure 5: Contact angle taken at the first instant the water dropped. (a) BPU nanocomposite with 0.0% silica; (b) BPU nanocomposite with 0.5% silica; (c) BPU nanocomposite with 1.0% silica; and (d) polypropylene (PP).

4. Conclusion

This study demonstrated the potential of castor oil-based polyurethane nanocomposite membranes as a promising alternative to fossil-derived polymers. The *in-situ* synthesis and incorporation of fumed silica nanoparticles enabled control over the morphology and physicochemical properties of the membranes, including pore distribution and hydrophobic characteristics. Notably, the 1.0% silica concentration led to a significant reduction in the maximum pore size (>80%) compared to the membrane containing 0.5% nanoparticles, highlighting the critical influence of silica loading on pore structure. Furthermore, nitrogen adsorption-desorption analysis revealed that BPU membranes exhibited behavior characteristic of mesoporous materials, whereas commercial polypropylene demonstrated macroporous characteristics. Water contact angle evaluation showed that hydrophobicity initially increased with the addition of silica (0.5%), but decreased at higher concentrations (1.0%) due to silica agglomeration, which impaired homogeneous dispersion and effective interactions within the composite. These findings underscore the viability of BPU membranes as functional materials for specific applications requiring tailored porosity and surface properties. Thus, integrating renewable materials into separation systems represents a significant contribution to the development of technologies aligned with circular economy principles and sustainability.

Acknowledgments

The authors gratefully acknowledge the support provided by grant #2015/20630-4 and grant #2017/11958-1 from the São Paulo Research Foundation (FAPESP), grant #140933/2023-9 from the Brazilian National Council for Scientific and Technological Development (Conselho Nacional de Desenvolvimento Científico e Tecnológico

- CNPq), and Prof. Dr. Celso Aparecido Bertran and Humberto Machado from the Functional Materials and Interfaces Laboratory (FMILab) at the Institute of Chemistry (Instituto de Química – IQ), UNICAMP, for their assistance with the DSA100 Drop Shape Analyzer.

References

Alothman, Z. A. (2012). A review: Fundamental aspects of silicate mesoporous materials. In *Materials* (Vol. 5, Issue 12, pp. 2874–2902).

Anovitz, L. M., & Cole, D. R. (2015). Characterization and analysis of porosity and pore structures. In *Pore Scale Geochemical Processes* (pp. 61–164). De Gruyter.

Asare, M. A., de Souza, F. M., Suthar, V. D., & Gupta, R. K. (2022). Nanocomposite-based flame-retardant polyurethane foams. In *Smart Polymer Nanocomposites: Design, Synthesis, Functionalization, Properties, and Applications* (pp. 543–569). Elsevier.

Assad, H., Sharma, S., Kaya, S., Sharma, P. K., & Kumar, A. (2023). Overview and fundamentals of polymer nanocomposites. In *Nanocomposites-Advanced Materials for Energy and Environmental Aspects* (pp. 41–66). Elsevier.

Bakhtiar, M., Ali, F., Ali, N., Saeed, S., Khan, M. M., Rtimi, S., Show, P. L., & Bilal, M. (2022). Silica-based polymer nanocomposites and their biomedical applications. In *Smart Polymer Nanocomposites: Design, Synthesis, Functionalization, Properties, and Applications* (pp. 507–528). Elsevier.

DeMeuse, M. T. (2021). Wet process for battery separator production. In *Polymer-Based Separators for Lithium-Ion Batteries* (pp. 71–91). Elsevier.

Gilbert, M. (2017). Relation of Structure to Chemical Properties. In *Brydson's Plastics Materials: Eighth Edition* (pp. 75–102). Elsevier Inc.

Khan, I., Khan, I., Saeed, K., Ali, N., Zada, N., Khan, A., Ali, F., Bilal, M., & Akhter, M. S. (2022). Polymer nanocomposites: an overview. In *Smart Polymer Nanocomposites: Design, Synthesis, Functionalization, Properties, and Applications* (pp. 167–184). Elsevier.

Kumar, A., Mishra, R. K., Verma, K., Aldosari, S. M., Maity, C. K., Verma, S., Patel, R., & Thakur, V. K. (2023). A comprehensive review of various biopolymer composites and their applications: From biocompatibility to self-healing. In *Materials Today Sustainability* (Vol. 23). Elsevier Ltd.

Kyzas, G. Z., & Mitropoulos, A. C. (2018). Adsorption domain theory. In *Composite Nanoadsorbents* (pp. 317–335). Elsevier.

Ma, Y., Zhu, X., Zhang, Y., Li, X., Chang, X., Shi, L., Lv, S., & Zhang, Y. (2024). Castor oil-based adhesives: A comprehensive review. In *Industrial Crops and Products* (Vol. 209). Elsevier B.V.

Nekhavhambe, E., Mukaya, H. E., & Nkazi, D. B. (2019). Development of castor oil–based polymers: A review. In *Journal of Advanced Manufacturing and Processing* (Vol. 1, Issue 4). John Wiley and Sons Inc.

Nishi, Y., & Inagaki, M. (2016). Gas Adsorption/Desorption Isotherm for Pore Structure Characterization. In *Materials Science and Engineering of Carbon: Characterization* (pp. 227–247). Elsevier.

Rajput, B. S., Samoylov, A. A., & Hai, T. A. P. (2023). Renewable, sustainable sources and bio-based monomers. In *Rethinking Polyester Polyurethanes: Algae Based Renewable, Sustainable, Biodegradable and Recyclable Materials* (pp. 67–91). Elsevier.

Singh, M. K., & Singh, A. (2022). Contact angle and surface wettability measurement. In *Characterization of Polymers and Fibres* (pp. 359–385). Elsevier.

Tripathi, N., Singh, A. S., Banshiwal, J. K., Pandey, P., & Bag, D. S. (2024). Effect of in-situ Incorporated Silica Particles on Properties of Polyurethane Elastomer. *Silicon*.

Zhang, Y., Shao, D., Yan, J., Jia, X., Li, Y., Yu, P., & Zhang, T. (2016). The pore size distribution and its relationship with shale gas capacity in organic-rich mudstone of Wufeng-Longmaxi Formations, Sichuan Basin, China. *Journal of Natural Gas Geoscience*, *1*(3), 213–220.

Zia, K. M., Akram, N., Tabasum, S., Noreen, A., & Akbar, M. U. (2021). Processing of bio-based polymers. In *Processing Technology for Bio-Based Polymers* (pp. 151–189). Elsevier.